Volume 61
Number 20
11 March 2025
Pages 3923–4080

ChemComm

Chemical Communications

rsc.li/chemcomm

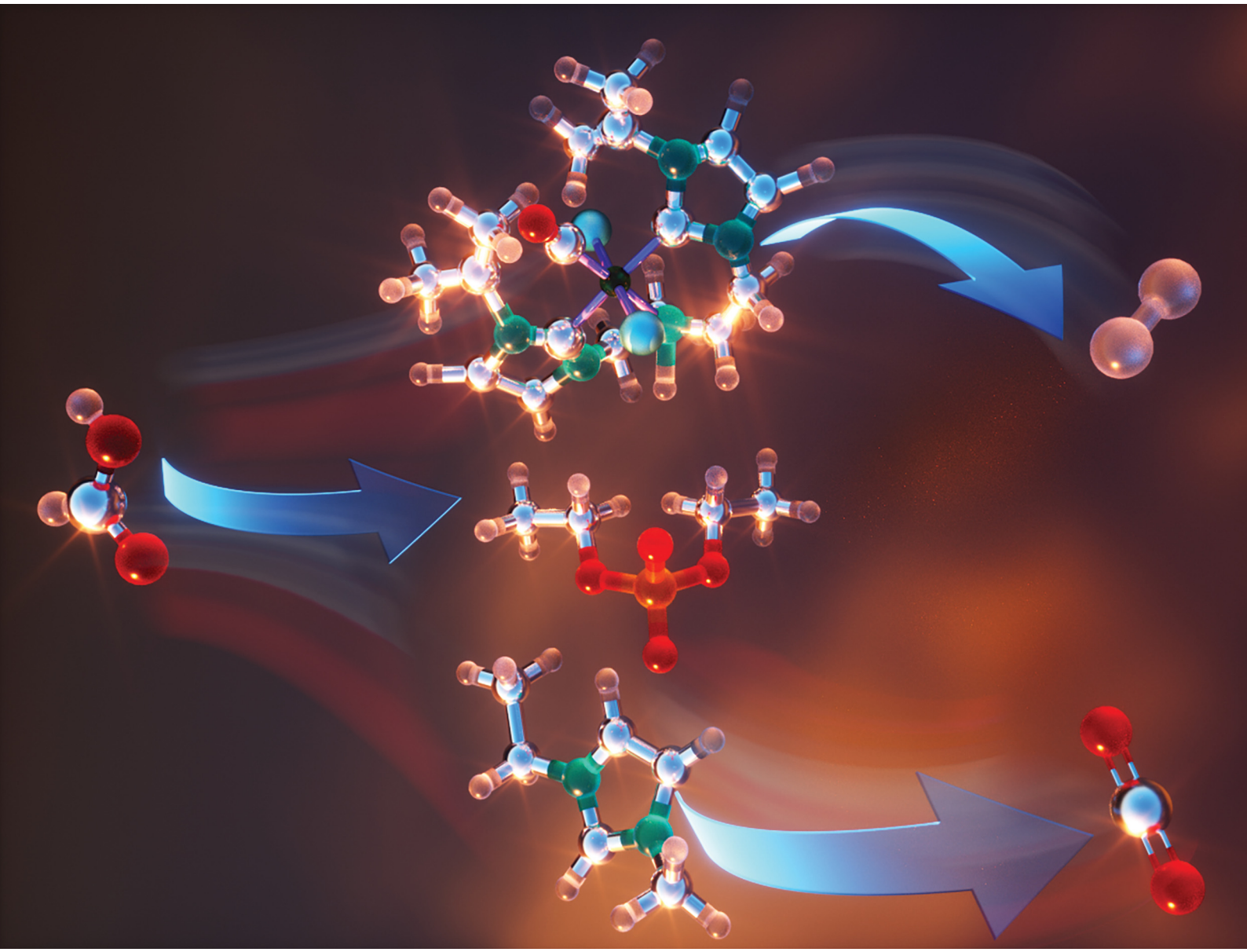

ISSN 1359-7345

ROYAL SOCIETY OF CHEMISTRY

COMMUNICATION

Mathias T. Nielsen, Martin Nielsen *et al.*
Formic acid dehydrogenation catalysed by a novel amino-di(N-heterocyclic carbene) based Ru-CNC pincer complex

ChemComm

COMMUNICATION

View Article Online
View Journal | View Issue

Cite this: *Chem. Commun.*, 2025, **61**, 3986

Received 1st October 2024,
Accepted 11th January 2025

DOI: 10.1039/d4cc05164e

rsc.li/chemcomm

Formic acid dehydrogenation catalysed by a novel amino-di(N-heterocyclic carbene) based Ru-CNC pincer complex†

Patricia Aufricht, Valeria Nori, Brenda Rabell, Luca Piccirilli, Sakhitha Koranchalil, René W. Larsen, Mathias T. Nielsen * and Martin Nielsen *

A new Ru(II) complex featuring a novel amino-di(N-heterocyclic carbene) CNC pincer ligand, ^{iPr}CNC-RuCl$_2$(CO) (Ru-1), has been developed and characterised in depth. Ru-1 forms an efficient and durable catalytic formic acid dehydrogenation system in combination with the ionic liquid 1-ethyl-3-methylimidazolium diethylphosphate (EMIM PO$_2$(OEt)$_2$).

Formic acid (FA) is considered a promising candidate for the long-term, safe, and practical chemical storage of hydrogen, serving as a platform compound to connect renewable energy and hydrogen fuel cells.[1–3] Formic acid dehydrogenation (FADH),[4] *i.e.*, the transformation of FA to H_2 and CO_2, has been demonstrated under mild conditions by numerous groups using a combination of transition metal (pre)catalyst, solvent, and additive.[5–11] For instance, using a Ru-PNP (PNP = phosphorous–nitrogen–phosphorous) pincer catalyst, in *N*,*N*′-dimethyl formamide (DMF) with amine bases, Pidko was able to achieve FADH with TON values of up to 706 500 at 90 °C.[6] A related mono Ir-complex was reported by Himeda to similarly facilitate FADH of an aqueous solution of FA with TON values of up to 10 000 000.[8] Sponholz, Junge, and Beller used the triazine-based Kempe Mn-PNP complex[9] for FADH in the presence of stoichiometric amounts of lysine in a 1 : 1 H_2O/THF mixture, achieving total TON values of 600 000 at 90 °C.[10] Milstein showed the first example of a homogeneous catalytic system capable of conducting FADH in neat FA.[11]

Apart from the latter example, many systems utilise (volatile) organic solvents in combination with additives, such as amine bases. While achieving high TONs, the presence of any volatile components necessitates further purification of the generated gas-mixtures. In this context, ionic liquids (ILs) represent a non-volatile alternative media for catalytic FADH,[12,13] and we recently started exploring their solvent properties for Ru-PNP[13a] and Ru-POP[13b] (POP = phosphorous–oxygen–phosphorous) catalysed FADH. ILs are a wide family of salts characteristic of a low melting point, a negligible vapor pressure, and a high chemical and thermal stability. Thus, using the commercially available Ru-MACHO-BH as catalyst in combination with the IL 1-butyl-3-methylimidazolium acetate (BMIM OAc) for FADH reached a TON exceeding 18 million and a durability of more than 110 days. Moreover, a large volume ratio between FA and IL exceeding 3600 was achieved, a desirable feature for application. When switching to Ru-POP pincer congeners, similar catalytic activities are observed for the short-term batch FADH systems.[13b] However, their durability is inferior, showing catalyst deactivation within several hours.

N-Heterocyclic carbenes (NHCs) are a group of ligands that are analogous to phosphines but exhibit certain desirable properties, such as the formation of thermodynamically stable metal–ligand bonds, which suggest that replacing phosphine groups with NHCs may lead to complexes demonstrating enhanced stability.[14–17] Especially pincer ligands bearing an amino-bridgehead are particularly interesting, as the bifunctionality of the amino-moiety renders metal–ligand cooperativity (MLC) possible. While a few other metal complexes bearing an (aliphatic) amino-based CNC (CNC = carbon (NHC)–nitrogen–carbon (NHC)) pincer ligand exist,[18–22] only two Ru-based complexes have been published by Pidko[23] and Masahiro and Yusuke,[24] both demonstrating high catalytic activity in carbonyl hydrogenation at low catalyst loadings.

Herein, we present the synthesis and characterisation of a Ru(II)-carbonyl dichlorido complex, ^{iPr}CNC-RuCl$_2$(CO) (**Ru-1**), bearing an amino-di(NHC) pincer ligand. We demonstrate that **Ru-1** in the IL 1-ethyl-3-methylimidazolium diethylphosphate (EMIM PO$_2$(OEt)$_2$) produces a highly active (and stable) catalytic system that enables full conversion of 200 equivalents of FA to CO_2 and H_2 within an hour at 100 °C, while also being tolerant towards exposure to air and multiple FA recharge additions without losing its catalytic activity. Furthermore, we show that

Department for Chemistry, Technical University of Denmark (DTU), 2800 Kongens Lyngby, Denmark. E-mail: mattni@kemi.dtu.dk, marnie@kemi.dtu.dk

† Electronic supplementary information (ESI) available. CCDC 2387750. For ESI and crystallographic data in CIF or other electronic format see DOI: https://doi.org/10.1039/d4cc05164e

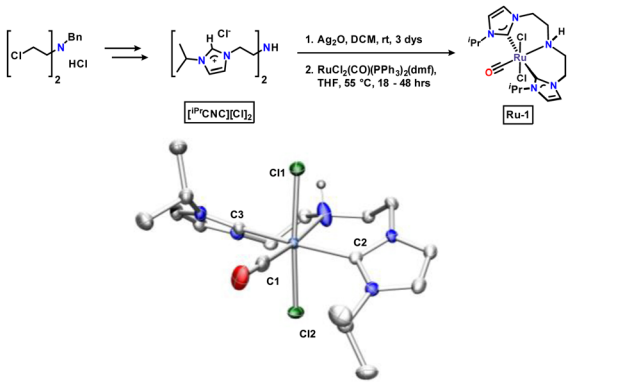

Scheme 1 Synthesis and solid-state of **Ru-1**. Thermal ellipsoid set at 50% probability level. All H atoms but the amino-bridgehead have been omitted for clarity. Colour scheme: H white, C grey, O red, N blue, Cl dark green, Ru dark blue. Selected interatomic distances (Å) and angles (°): Ru–C1 1.817(4); Ru–C2 2.105(3); Ru–N 2.247(3); Ru–C3 2.096(3); Ru–Cl1 2.4188(7); Ru–Cl2 2.4319(7); C1–O 1.149(5); C1–Ru–N 173.62(14); C2–Ru–C3 173.21(11); Cl1–Ru–Cl2: 175.35(3).

Table 1 Optimisation of reaction parameters for **Ru-1** catalysed FADH in EMIM OAc[a]

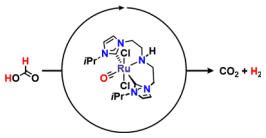

Entry	IL	**Ru-1** [mol%]	Temp. [°C]	Conv.[b] [%]	TON	TOF_{max} [h^{-1}]
1	None	0.1	80	<5	—	—
2	None	0.1	90	<5	—	—
3	EMIM OAc	0.1	80	83	830	670
4	EMIM OAc	0.1	90	91	910	1480
5	EMIM OAc	0.1	100	94	930	2650
6	EMIM OAc	0.05	90	86	1730	1630
7	EMIM OAc	0.025	90	73	2940	2010
8	EMIM OAc	0.05	100	90	1800	3500

[a] Standard reaction conditions: **Ru-1** (0.025–0.1 mol%), IL (1 mL), FA (0.5 mL, 13.25 mmol), 3 h under gentle flow of Ar. Gas composition is analysed by GC-TCD. [b] Determined by ^{1}H-NMR.

the IL EMIM $PO_2(OEt)_2$ is a superior reaction medium to the acetate-based IL 1-ethyl-3-methylimidazolium acetate (EMIM OAc) for **Ru-1** catalysed FADH.

Starting from *N*-benzyl-bis(2-chloroethyl) amine hydrochloride, **[^{iPr}CNC][Cl]$_2$** is isolable in excellent yield (90%, Scheme 1). Transmetalation of **[^{iPr}CNC][Cl]$_2$** *via* an Ag-masked carbene with $RuCl_2(CO)(PPh_3)_2(dmf)$[25] in THF affords **Ru-1** as yellow crystals in an acceptable yield of up to 40%. The NHC precursor was obtained by reacting **[^{iPr}CNC][Cl]$_2$** to Ag_2O in DCM, which yields a light-sensitive orange/brown material that features a ^{1}H nuclear magnetic resonance (NMR) and ^{13}C-NMR spectra consistent with a heteroleptic NHC-Ag–Cl species, see Fig. S5–S7 (ESI†).[19] **Ru-1** was characterised in the solid state by single-crystal X-ray diffraction (SC-XRD) and infrared-spectroscopy (IR), and in solution by high-resolution mass-spectrometry (HRMS) as well as 1D and 2D multinuclear NMR spectroscopy, including ^{1}H, ^{13}C, ^{31}P, {^{1}H–^{1}H} COSY, as well as {^{1}H–^{13}C} HSQC and HMBC. **Ru-1** crystallises in the monoclinic $P2_1/c$ space group and exhibits a slightly distorted octahedral coordination environment of Ru, as depicted in Scheme 1. The CNC pincer ligand coordinates in a meridional fashion and features a carbonyl ligand *trans* to the amino-bridgehead. The Ru–C bond lengths belonging to the two NHCs are 2.096(3) and 2.105(3) Å, respectively, and the Ru–C bond length of Ru–CO is 1.817(4) Å. These bond lengths are comparable to those reported by Masahiro and Yusuke.[24] Solution-state ^{1}H and ^{13}C NMR of **Ru-1**, Fig. S9–S14 (ESI†), are consistent with the solid-state structure. In the ^{13}C-NMR spectrum, the two most downfield-shifted signals are consistent with the C atom of the carbonyl ligand (208.8 ppm) and the C_2 atom of the NHCs (184.0 ppm). {^{1}H–^{13}C} HMBC delineates these two signals from one another, as only the latter signal demonstrates a cross-peak with the imdazole-2-ylidene C_4/C_5-protons. Importantly, no residual triphenylphosphine is observed *via* ^{31}P-NMR spectroscopy.

With **Ru-1** in hand, we investigated its potential use as a (pre)catalyst for FADH. While **Ru-1** does not catalyse FADH in neat FA (Table 1, entries 1 and 2), using EMIM OAc as solvent afforded 83% FA conversion (TOF_{max} = 670 h^{-1}) at 80 °C after 3 hours with a low loading of **Ru-1** (0.1 mol%, entry 3). Increasing the temperature to 90 °C and to 100 °C, afforded conversions of 91% and 94%, respectively, and significantly enhanced TOF_{max} values of 1480 h^{-1} and 2650 h^{-1}, respectively (entries 4 and 5). As depicted in Fig. S15 (ESI†), FADH conversion with **Ru-1** in EMIM OAc operating at temperatures below 100 °C clearly has an induction phase. Despite this induction period, **Ru-1** continues to effectively catalyse FADH even when the loading is reduced from 0.1 mol% to 0.05 mol% and further to 0.025 mol%, resulting in 86% and 73% conversion after 3 hours, respectively, at 90 °C (entries 6 and 7). Despite the incomplete FA consumption within the set time frame, high TON (2940) and TOF_{max} (2010 h^{-1}) values were recorded. The same behaviour was observed at 100 °C when decreasing the loading to 0.5 mol%, with TON = 1800 and TOF_{max} = 3500 h^{-1} (entry 8).

Contrasting our previous work on FADH where acetate-based ILs were employed with various catalysts,[13] using EMIM OAc in combination with **Ru-1** does not afford complete conversion within a reasonable timeframe such as 3 hours. We speculate that this is due to **Ru-1** forming off-cyclic acetato-adducts in acetate-based ILs when FA concentration is sufficiently low (vide infra). Hence, we turned our attention to EMIM $PO_2(OEt)_2$, and pleasingly observed full FA conversion at 90 °C, see Table 2, entry 3. However, as evident in the TOF_{max} values, there is a marked difference in the initial rate between the two ILs, see Fig. S16 (ESI†).

Subsequent screening of reaction conditions of the phosphate-based IL system revealed that at 100 °C, full conversion was achieved within one hour resulting in a TOF_{max} of 1100 h^{-1} (entry 4). Lowering the loading of **Ru-1** to 0.05 mol% still achieved full conversion albeit only after 3 hours, providing a TON of 2000 and TOF_{max} of 820 h^{-1} (entry 5).

We then studied the durability of **Ru-1** over multiple FADH cycles with various loadings of FA. Successively supplying the

Table 2 Ionic liquid screening for FADH optimisation with **Ru-1**[a]

Entry	IL	**Ru-1** [mol%]	Temp. [°C]	Conv.[b] [%]	TON	TOF_{max} [h^{-1}]
1	EMIM OAc	0.1	90	91	910	1480
2	EMIM OAc	0.05	90	86	1730	1630
3	EMIM $PO_2(OEt)_2$	0.1	90	>99	1000	400
4	EMIM $PO_2(OEt)_2$	0.1	100	>99	1000	1100
5	EMIM $PO_2(OEt)_2$	0.05	100	>99	2000	820

[a] Standard reaction conditions: **Ru-1** (0.05–0.1 mol%), IL (1 mL), FA (0.5 mL, 13.25 mmol), 3 h under gentle flow of Ar. Gas composition is analysed by GC-TCD. [b] Determined by ^{1}H-NMR.

setup with FA still led to full conversion after six cycles, after which no more cycles were attempted (see Fig. 1 and Table S21, ESI†). Furthermore, leaving the reaction medium standing for three days between cycles 2 and 3 has practically no influence on its catalytic performance. In addition, in cycle 4 the amount of supplied FA was doubled which considerably slowed down the FADH activity in the first hour (approximately 20% conversion) but nevertheless led to 85% conversion after 3 hours and full conversion after 4 hours. Hence, there seems to be a saturation point of FA in EMIM $PO_2(OEt)_2$ after which the beneficial effect of the IL on the catalytic activity of activated **Ru-1** diminishes significantly but can be regained once sufficient FA has been converted (at a slower rate). Notably, full FA conversion is repeatedly reached in the following two cycles as well (cycle 5 and 6), and all six cycles proceed with similar TOF_{max} values (490–650 h^{-1}), indicating that the combination of **Ru-1** and EMIM $PO_2(OEt)_2$ comprises a stable and durable catalytic system for FADH.

In situ HR-MS and ^{1}H-NMR spectroscopy (Fig. S17–S19, ESI†) show early formation of a formato species in cycle 1 during the slow onset of catalysis and the appearance of a hydrido species after two cycles. This is in line with the expectation that **Ru-1** is a precatalyst, the formato complex an off-cycle species, and the hydrido complex the resting state. **Ru-1** is proposed to turn into the amido congener by HCl elimination, likely facilitated by the IL anion. In the same manner, the formato complex turns into the amido congener by FA elimination. Furthermore, FA dehydrogenation is proposed to occur on the amido complex *via* an outer sphere mechanism. Moreover, EMIM OAc seems more efficient than EMIM $PO_2(OEt)_2$ at generating the amido species, but also coordinates to the catalyst, a particular obstacle at low FA concentration. On the other hand, the use of phosphate-based ILs might be superior to acetate-based ones due to a lower propensity to compete with formato complex formation. This also explains the slow FADH with doubled FA addition in EMIM $PO_2(OEt)_2$.

Having demonstrated the resilience of **Ru-1** and EMIM $PO_2(OEt)_2$, we sought to assess the influence of the CNC pincer ligand. To this end, we carried out the successive cycles using two related Ru(II) carbonyl complexes typically considered as simple metal precursors, *i.e.*, $RuCl_2(CO)(PPh_3)_2$(dmf) and $RuHCl(CO)(PPh_3)_3$.

Fig. 2 shows the FA conversion for four of six successive cycles, comparing **Ru-1** to the two precursors where the inserts **A**, **B**, **C**, and **D**, show the first, second, fifth, and sixth batch cycle, respectively. See Fig. S25–S29 and Tables S15–S34 (ESI†) for relevant data on gas composition, comparison of FADH efficacy of the individual precursor over six batches as well as compared with **Ru-1**, and listings of TON/TOF values. Surprisingly, in the first cycle (insert **A**), both precursors, but particularly $RuCl_2(CO)(PPh_3)_2$(dmf), demonstrated markedly better catalytic activity than **Ru-1**. Interestingly, *in situ* ^{1}H NMR

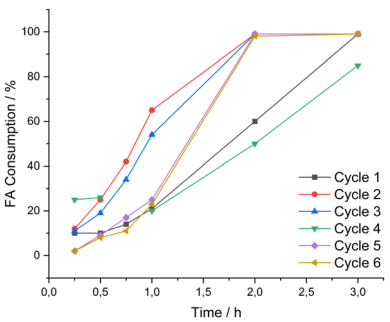

Fig. 1 FA conversion over time in batch reactions conducted in EMIM $PO_2(OEt)_2$ using **Ru-1** as (pre)catalysts. In cycle 4 an excess of FA is purposefully added to the system. It shows a similar conversion to the first cycle.

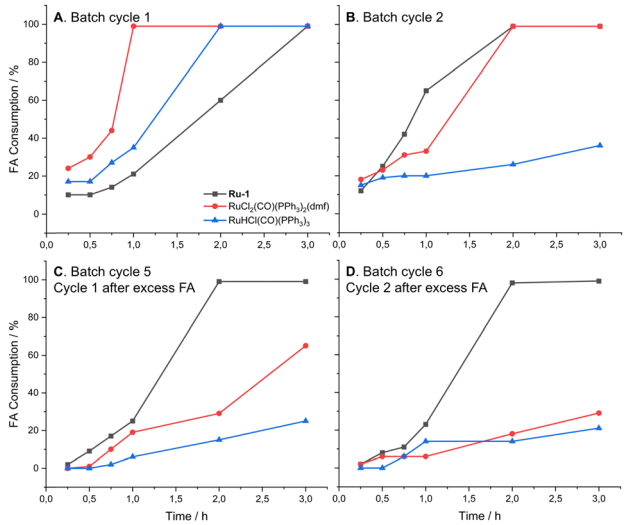

Fig. 2 FA conversion over time in batch reactions conducted in EMIM $PO_2(OEt)_2$ comparing **Ru-1**, $RuCl_2(CO)(PPh_3)_2$(dmf), and $RuHCl(CO)(PPh_3)_3$ as (pre)catalysts. Insert **A** and **B** show the first and second batch cycles, respectively. Insert **C** and **D** show the fifth and sixth cycles, which correspond to the first and second cycle after the introduction of an excess of FA.

analysis before complete FA consumption (45 min reaction time) revealed the formation of several hydrido species in the two precursor systems, with one species appearing to be dominant in both systems, see Fig. S18a (ESI†). In addition, *in situ* HR-MS analysis suggests the incorporation of an EMIM-based NHC-ligand into the ligand system of both precursors, see Fig. S19a–d (ESI†). However, these catalytically active species seem to degrade over time, possibly due to an instability at elevated temperature in the absence of FA. This is also evident from the second FADH cycle (insert **B**), where $RuHCl(CO)(PPh_3)_3$ exhibited poor catalytic conversion and $RuCl_2(CO)(PPh_3)_2(dmf)$ has become similar to **Ru-1** in activity. Furthermore, oversaturating the systems with FA in cycle 4 leads to much lower conversions in cycles 5 and 6 (inserts **C** and **D**, respectively), demonstrating that the precursors are significantly inferior to **Ru-1**. These observations support that the use of a CNC pincer ligand imposes stability for FADH catalysis in EMIM $PO_2(OEt)_2$.

In conclusion, we have developed a novel amino-based di(NHC) Ru pincer complex, **Ru-1**, and fully characterised it by a range of analytical techniques, including SC-XRD, IR, NMR, and MS. **Ru-1** in combination with the IL EMIM $PO_2(OEt)_2$ results in a catalytic system that enables efficient and durable FADH under mild conditions, producing only H_2 and CO_2 gas. Additionally, the system can withstand exposure to an excess of FA without incurring significant loss in catalytic capabilities over several cycles, different from two Ru(II) precursors. *In situ* analysis of the catalytic reactions reveals the appearance of formato and hydrido species, indicating that **Ru-1** undergoes initial activation, suggesting that phosphate-based ILs might be better than acetate-based ones due to a reduced tendency to generating off-cycle complexation with the catalyst.

The authors are grateful to the Independent Research Fund Denmark (8102-00330B and 1113-00027B), VILLUM FONDEN (19049 and 53069), and Carlsberg Foundation (CF20-0365) for generous funding. P. A. Thanks the Erasmus+ programme of the European Union (2023-1-DE01-KA131-HED-000120711). L. P. Thanks Otto Mønsted (22-55-0557), Brødrene Hartmanns Foundation (A37.412), and DTU Discovery Grant.

Data availability

The data supporting this article have been included as part of the ESI.†

Conflicts of interest

There are no conflicts to declare.

References

1 C. Fellay, P. J. Dyson and G. Laurenczy, *Angew. Chem., Int. Ed.*, 2008, **47**, 3966–3968.
2 B. Loges, A. Boddien, H. Junge and M. Beller, *Angew. Chem., Int. Ed.*, 2008, **47**, 3962–3965.
3 C. Guan, Y. Pan, T. Zhang, M. J. Ajitha and K.-W. Huang, *Chem. – Asian J.*, 2020, **15**, 937–946.
4 (*a*) K. Müller, K. Brooks and T. Autrey, *Energy Fuels*, 2017, **31**, 12603–12611; (*b*) J. Guo, C. K. Yin, D. L. Zhong, Y. L. Wang, T. Qi, G. H. Liu, L. T. Shen, Q. S. Zhou, Z. H. Peng, H. Yao and X. B. Li, *ChemSusChem*, 2021, **14**, 2655–2681; (*c*) D. Mellmann, P. Sponholz, H. Junge and M. Beller, *Chem. Soc. Rev.*, 2016, **45**, 3954–3988; (*d*) A. Wang, P. He, J. Wu, N. Chen, C. Pan, E. Shi, H. Jia, T. Hu, K. He, Q. Cai and R. Shen, *Energy Fuels*, 2023, **37**, 17075–17093; (*e*) L. Piccirilli, D. L. J. Pinheiro and M. Nielsen, *Catalysts*, 2020, **10**, 773; (*f*) S. Patra, B. Maji, H. Kawanami and Y. Himeda, *RSC Sustainability*, 2023, **1**, 1655–1671; (*g*) M. H. G. Prechtl and S. Sahler, *Curr. Org. Chem.*, 2013, **17**, 220–228; (*h*) K. Sordakis, C. Tang, L. K. Vogt, H. Junge, P. J. Dyson, M. Beller and G. Laurenczy, *Chem. Rev.*, 2018, **118**, 372–433.
5 E. A. Bielinski, P. O. Lagaditis, Y. Zhang, B. Q. Mercado, C. Würtele, W. H. Bernskoetter, N. Hazari and S. Schneider, *J. Am. Chem. Soc.*, 2014, **136**, 10234–10237.
6 G. A. Filonenko, R. van Putten, E. N. Schulpen, E. J. M. Hensen and E. A. Pidko, *ChemCatChem*, 2014, **6**, 1526–1530.
7 J. F. Hull, Y. Himeda, W.-H. Wang, B. Hashiguchi, R. Periana, D. J. Szalda, J. T. Muckerman and E. Fujita, *Nat. Chem.*, 2012, **4**, 383–388.
8 N. Onishi, R. Kanega, E. Fujita and Y. Himeda, *Adv. Synth. Catal.*, 2019, **361**, 289–296.
9 S. Rösler, M. Ertl, T. Irrgang and R. Kempe, *Angew. Chem., Int. Ed.*, 2015, **54**, 15046–15050.
10 D. Wei, R. Sang, P. Sponholz, H. Junge and M. Beller, *Nat. Energy*, 2022, **7**, 438–447.
11 S. Kar, M. Rauch, G. Leitus, Y. Ben-David and D. Milstein, *Nat. Catal.*, 2021, **4**, 193–201.
12 (*a*) A. Moazezbarabadi, D. Wei, H. Junge and M. Beller, *ChemSusChem*, 2022, **15**, e202201502; (*b*) J. D. Scholten, M. H. G. Prechtl and J. Dupont, *ChemCatChem*, 2010, **2**, 1177–1327; (*c*) X. Li, X. Ma, F. Shi and Y. Deng, *ChemSusChem*, 2010, **3**, 71–74.
13 (*a*) L. Piccirilli, B. Rabell, R. Padilla, A. Riisager, S. Das and M. Nielsen, *J. Am. Chem. Soc.*, 2023, **145**, 5655–5663; (*b*) A. T. Nikol, B. Rabell, M. S. B. Jørgensen, R. W. Larsen and M. Nielsen, *Sci. Rep.*, 2024, **14**, 26209.
14 W. A. Herrmann, *Angew. Chem., Int. Ed.*, 2002, **41**, 1290–1309.
15 F. E. Hahn and M. C. Jahnke, *Angew. Chem., Int. Ed.*, 2008, **47**, 3122–3172.
16 H. Jacobsen, A. Correa, A. Poater, C. Costabile and L. Cavallo, *Coord. Chem. Rev.*, 2009, **253**, 687–703.
17 S. Díez-González, N. Marion and S. P. Nolan, *Chem. Rev.*, 2009, **109**, 3612–3676.
18 R. Zhong, Z. Wei, W. Zhang, S. Liu and Q. Liu, *Chem*, 2019, **5**, 1552–1566.
19 J. Houghton, G. Dyson, R. E. Douthwaite, A. C. Whitwood and B. M. Kariuki, *Dalton Trans.*, 2007, 3065–3073.
20 C.-F. Yang, T. Lu, X.-T. Chen and Z.-L. Xue, *Chem. Commun.*, 2018, **54**, 7830–7833.
21 W. B. Cross, C. G. Daly, R. L. Ackerman, I. R. George and K. Singh, *Dalton Trans.*, 2011, **40**, 495–505.
22 W. Wei, Y. Qin, M. Luo, P. Xia and M. S. Wong, *Organometallics*, 2008, **27**, 2268–2272.
23 G. A. Filonenko, M. J. B. Aguila, E. N. Schulpen, R. van Putten, J. Wiecko, C. Müller, L. Lefort, E. J. M. Hensen and E. A. Pidko, *J. Am. Chem. Soc.*, 2015, **137**, 7620–7623.
24 M. Yusuke and T. Masahiro, *US Pat.*, US2016145282A1, 2016.
25 V. Gómez-Benitez, J. Olvera-Mancilla, S. Hernández-Ortega and D. Morales-Morales, *J. Mol. Struct.*, 2004, **689**, 137–141.